ELECTRONIC SUPPORTING INFORMATION

Diverse isostructural MOFs by postsynthetic metal node metathesis: anionic-to-cationic framework conversion, luminescence and separation of dyes

Soana Seth, Govardhan Savitha and Jarugu NarasimhaMoorthy*

Department of Chemistry, Indian Institute of Technology Kanpur, Kanpur 208016, INDIA

Table of Contents

General Aspects

^{1}H NMR spectra were recorded on JEOL-Lambda (400 MHz and 500 MHz) spectrometers with deuterated chloroform or DMSO as an internal standard. ^{13}C NMR spectra were recorded with 125 MHz NMR spectrometer with complete proton decoupling. IR spectra were recorded with a Bruker Vector 22 FT-IR spectrophotometer. Mass spectral analyses were carried out with Waters ESI-Q^{TOF} Instrument. The melting points were determined with a JSGW melting point apparatus. Column chromatography was conducted with silica-gel 100-200 μ mesh (Souvenier Chemicals, India). All the solvents were freshly distilled prior to use. All metal salts, dyes and DMF (*N,N*-dimethylformamide) were obtained from Sigma-Aldrich and Alfa Aesar, and were used as received. The single crystal X-ray diffraction data were collected on a Bruker SMART/CCD diffractometer using MoKα radiation. Powder X-ray diffraction measurements were recorded on a Rigaku X-ray diffractometer. Thermal analyses (N_2 atmosphere, heating rate of 10 °C/min) were carried out in a Mettler Toledo TGA equipment. Energy dispersive X-ray spectroscopy (EDX) was carried out with a JEOL-7500F Microscope equipped with an energy–dispersive spectroscopy (EDS) instrument. ICP-AES analyses were performed with ICP-9000(N+M) (USA Thermo Jarrell-Ash Corp).

X-Ray Crystal Structure Determinations

A good quality crystal in the case was chosen, mounted on a glass capillary, and the intensity data was collected at 100 K on a Bruker Nonius SMART APEX CCD detector system with Mo-sealed Siemens ceramic diffraction tube (λ = 0.71073) and a highly oriented graphite monochromator operating at 50 kV and 30 mA. The data were collected on a hemisphere mode and processed with Bruker SAINTPLUS. Empirical absorption correction was made using Bruker SADABS. The structures were solved by Direct Methods using SHELXTL package and refined by full matrix least squares method based on F^2 using SHELX97 program. All the non-hydrogen atoms were refined anisotropically. The hydrogen atoms were fixed in their ideal positions, assigned fixed isotropic U values and allowed to ride with their respective non-hydrogen atoms. The details of crystal data, structure solution and refinement are presented in Tables S3 to S6.

Synthesis of the Tetraacid Ligand H_4L.

Synthesis of 3,3',5,5'-Tetrakis(*p*-methylphenyl)-2,2',6,6'-tetramethoxy-1,1'-biphenyl. A two-

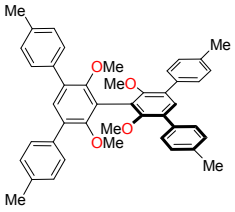

necked RB flask was charged with dioxane (15 mL) and water (15 mL), and the mixture was degassed and bubbled with N_2 for 15 min. Subsequently, 3,3',5,5'-tetraiodo-2,2',6,6'-tetramethoxy-1,1'-biphenyl (2.0 g; 2.56 mmol), *p*-methylphenylboronic acid (13.4 g; 25.68 mmol) and NaOH (1.0 g; 25.68 mmol) were added to the round bottom flask followed by addition of the catalyst $Pd(PPh_3)_4$ (0.2 g; 0.24 mmol). The entire mixture was heated at reflux for 2 d. At the end of this period, dioxane was removed in vacuo and the residue was extracted with chloroform for two times. The combined organic extract was dried with anhydrous Na_2SO_4 and the solvent was removed in vacuo to obtain the crude product, which was purified by column chromatography to obtain 1.4 g (88%) of the product, mp 230-232 °C; IR (solid) cm^{-1} 3431, 29381462, 1060; ^1H NMR ($CDCl_3$, 500 MHz) δ 2.40 (s, 12H), 3.39 (s, 12H), 7.22 (d, J = 7.8 Hz, 8H), 7.38 (s, 2H), 7.52 (d, J = 7.8 Hz, 8H); ^{13}C NMR ($CDCl_3$, 125 MHz) δ 21.2, 60.3, 124.1, 128.9, 129.0, 130.2, 132.3, 135.8, 136.5, 155.4; ESI-MS^+ m/z Calcd for $C_{44}H4_2O_4Na$ 657.2980 $[M + Na]^+$, found 657.2986.

Synthesis of 3.3',5,5'-Tetrakis(*p*-carboxyphenyl)-2,2',6,6'-tetramethoxy-1,1'-biphenyl, H_4L.

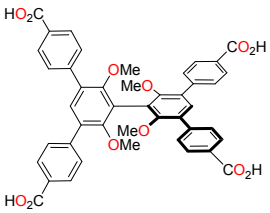

3,3',5,5'-Tetrakis(*p*-tolyl)-2,2',6,6'-tetramethoxy-1,1'-biphenyl (1.0 g; 1.58 mmol) was taken in a mixture of pyridine (32 mL) and H_2O (8 mL). $KMnO_4$ (2.50 g; 15.8 mmol) was added to the reaction and heated at reflux for 6 days. $KMnO_4$ was added in increments at regular intervals of time and the reaction was monitored by TLC analysis. After completion of the reaction as judged from TLC analysis, pyridine was removed in vacuo, the brown solid was filtered off and washed with water. The filtrate was acidified with conc. HCl, and the resulting precipitate was collected by filtration to

afford 0.80 g (67%) of the final tetracarboxylic acid, mp (decomp) 272-274 °C; IR (solid) cm^{-1} 3414, 2943, 2662, 1687; ^{1}H NMR (CD_3OD, 500 MHz) δ 3.40 (s, 12H), 7.52 (s, 2H), 7.75 (d, J = 8.5 Hz, 8H), 8.11 (d, J = 8.5 Hz, 8H); ^{13}C NMR $(CD_3)_2SO$, 125 MHz) δ 60.5, 123.9, 128.9, 129.3, 129.6, 142.1, 155.9, 167.2; ESI-MS m/z Calcd for $C_{44}H_{33}O_{12}$ 753.1972 $[M-H]^-$, found 753.1974.

Synthesis of Cd-MOFs

Synthesis of Cd-MOF4. The tetraacid ligand **H_4L** (0.01 g, 0.013 mmol) and $Cd(NO_3)_2$ (0.013 g, 0.053 mmol) were dissolved in 1.5 mL of DMF taken in a 5 mL culture tube. The solution was heated for 48 h in a sand-bath placed in an oven maintained at 90 °C. After this period, the temperature was allowed to slowly attain to room temperature. Colourless block-shaped crystals were isolated by filtration, washed thoroughly with DMF and allowed to air dry. (11.6 mg, 47.4%).

Cd-MOF1, Cd-MOF2, Cd-MOF8 and Cd-MOF12 were synthesized by following the same procedure used for the synthesis of **Cd-MOF4**, but by varying the ligand, i.e., $Cd(NO_3)_2$, mole ratio. Accordingly, **H_4L** and $Cd(NO_3)_2$ were employed in 1:1, 1:2, 1:8 and 1:12 ratios.

Typical procedure of metal exchange. The crystals of the **Cd-MOF1** (ca. 10.0 mg) were suspended in 1 mL 0.01 M solutions of different metal salts in DMF. The mother liquor in each case was replenished by a fresh solution of the metal salt every 3 days once. After 15-20 days, the crystals were filtered and washed thoroughly with DMF to remove the organic and inorganic materials adsorbed at the surface. Finally, the metal-organic materials were allowed to dry. The material thus derived was examined by ICP-AES and EDX to determine the magnitude of metal exchange in each case.

Reversibility of PSME

The reversibility of PSME was investigated for one metal ion of each of lanthanides, transition metal ions and main group metal ions; specifically, the cases for which the exchange was found to be more than 90% after soaking the crystals for 25 days were chosen for these investigations. Typically, ca. 20 mg **Cd-MOF** was soaked in 1mL each of 0.01 M solution of $Tb(NO_3)_3$, $SrCl_2$ and $ZnCl_2$ in DMF. The solutions were replenished by respective fresh solutions every two days. After 10 days, half of the crystals in each case were taken out, washed several times for getting rid of the excess metal ions and allowed to dry prior to ICP-AES analyses. The other parts of the crystals were subjected to the reverse exchange with 0.01 M $Cd(NO_3)_2$ solution in the same manner for 10 days. The ratios of the metal ions as determined from the ICP-AES analyses are collated in Table S2. The reversibility of the process in all cases and the high propensity for the exchanged metal ions to be substituted again by Cd(II) ions clearly indicates that the **Cd-MOF** is highly robust and that the exchange of the framework metal ions occurs mostly due to the flexibility of the framework as well as concentration gradient.

Table S1. M:Cd atomic ratio of the MOFs after forward and reverse metal exchange for 10 days.

Code	**M/Cd atomic ratio (ICP-AES)**
Tb@MOF forward	39.6: 60.4
Tb@MOF reverse	4.5: 95.5
Sr@MOF forward	99.8 : 0.2
Sr@MOF reverse	0.08: 99.02
Zn@MOF forward	56.4: 43.6
Zn@MOF reverse	5.6: 94.4

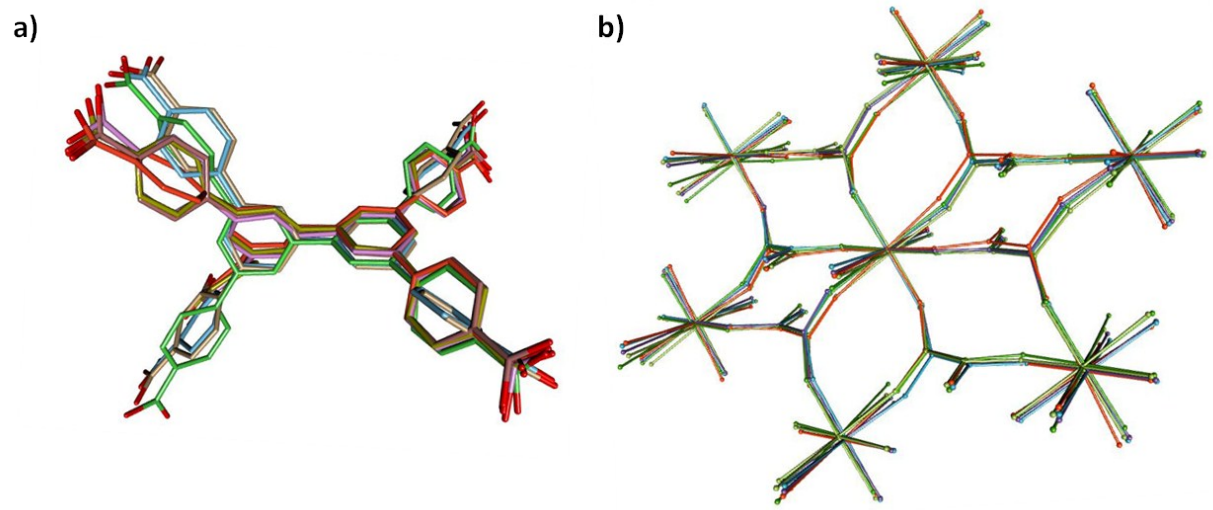

Figure S1. An overlay of (a) the structures of ligand **L** and (b) framework structures (as a 3,8-connecting net) observed in the five Cd-MOFs, viz., **Cd-MOF-1**, **Cd-MOF-2**, **Cd-MOF-4**, **Cd-MOF-8**, and **Cd-MOF-12**.

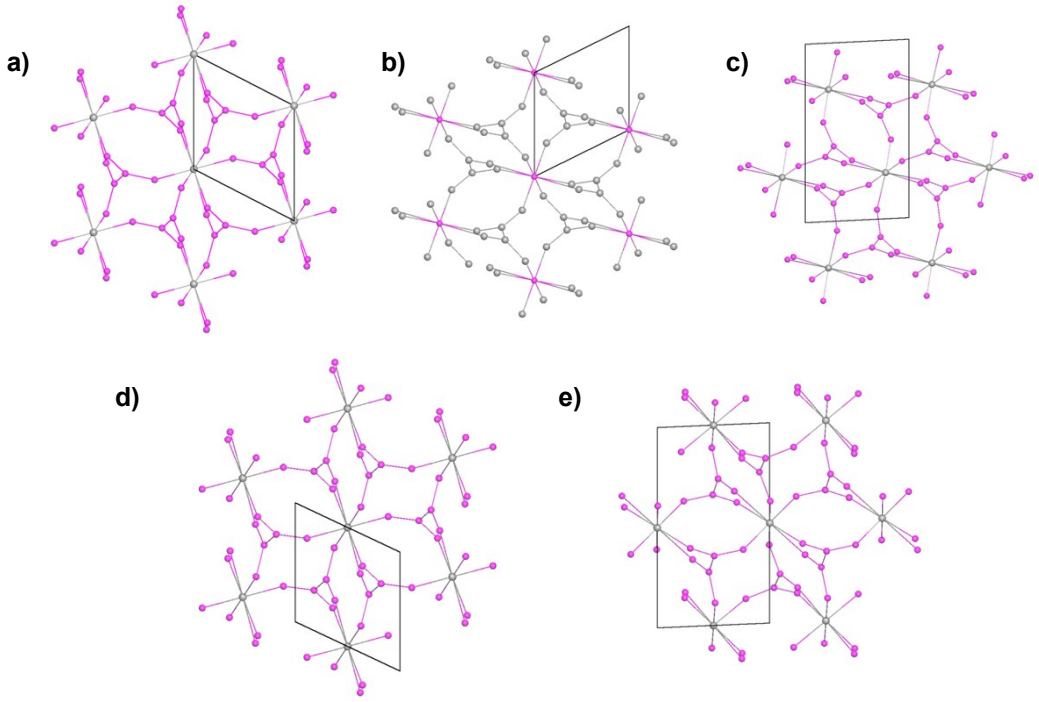

Figure S2. The crystal packing diagrams of all **Cd-MOF**s, i.e., **Cd-MOF-1**, **Cd-MOF-2**, **Cd-MOF-4**, **Cd-MOF-8**, and **Cd-MOF-12,** by reducing the ligand to a pair of 3-connecting module (a-e). Note that the coordination mode and basic organization are similar in each case. Cell parameters are defined differently for each of them due to small changes in the overall structure.

Table S2. Torsional angles between the dimethoxyaryl rings (**φ**), and the phenylcarboxylate rings and the dimethoxyaryl rings of $\mathbf{L^{4-}}$ in the Cd-MOFs.

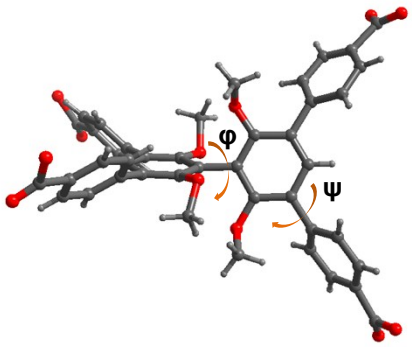

Cd-MOF	φ	ψ	Cell volume (Å^3)
Cd-MOF1	72.032	43.128, 49.53, 49.194, 82.854	3731.08
Cd-MOF2	63.559	44.26, 49.363, 60.982, 49.076	3483.56
Cd-MOF4	70.601, 65.453	63.099, 50.701, 45.386, 45.722; 57.84, 55.565, 42.775, 51.803	7465.95
Cd-MOF8	72.613	47.334, 46.250, 48.803, 71.273	3844.03
Cd-MOF12	73.330, 71.752	50.792, 57.535, 48.777, 49.024; 52.197, 55.392, 43.503, 49.179	7588.83

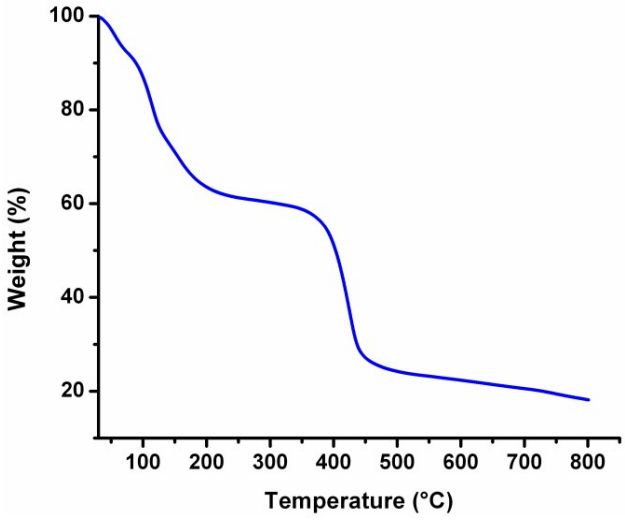

Figure S3. TGA profile of **Cd-MOF4**. The sample was heated from 30 °C to 800 °C at a heating rate of 10 °C/min.

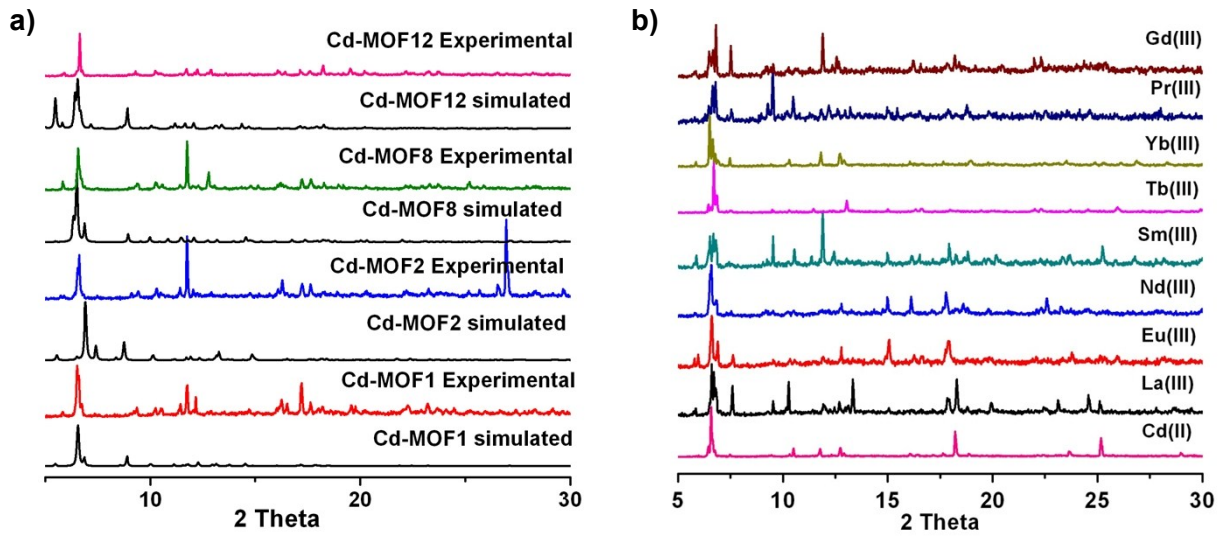

Figure S4. (a) PXRD profiles of **Cd-MOF1**, **Cd-MOF2**, **Cd-MOF8** and **Cd-MOF12** with their theoretically simulated profiles based on their single crystal structures. (b) PXRD profiles Ln@MOFs compared with the PXRD of as synthesized **Cd-MOF**.

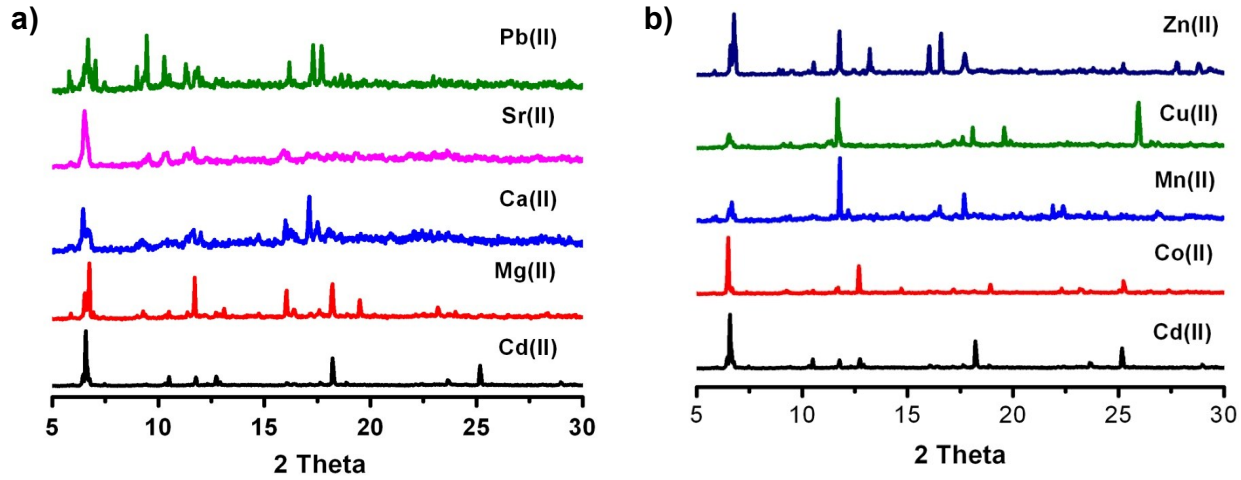

Figure S5. PXRD profiles of the (a) **Mm@MOF**s (main group metal ions) and (b) **Tm@MOF**s (transition metal ions) as compared to that of the parent **Cd-MOF**.

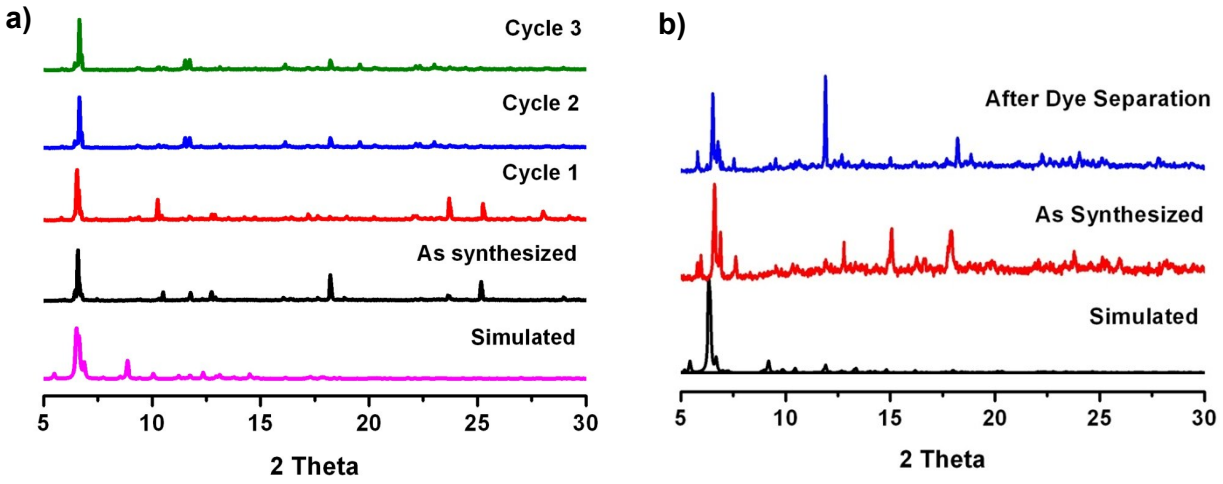

Figure S6. (a) PXRD profiles of as-synthesized **Cd-MOF4**, after 1st, 2nd and 3rd cycles of dye adsorption study and their comaprison with the simulated pattern obtained from single crystal structure determination. (b) PXRD of **Eu@MOF** after the dye adsorption study as compared to that of the as-synthesized **Eu@MOF** and the simulated profile from the single crystal structure.

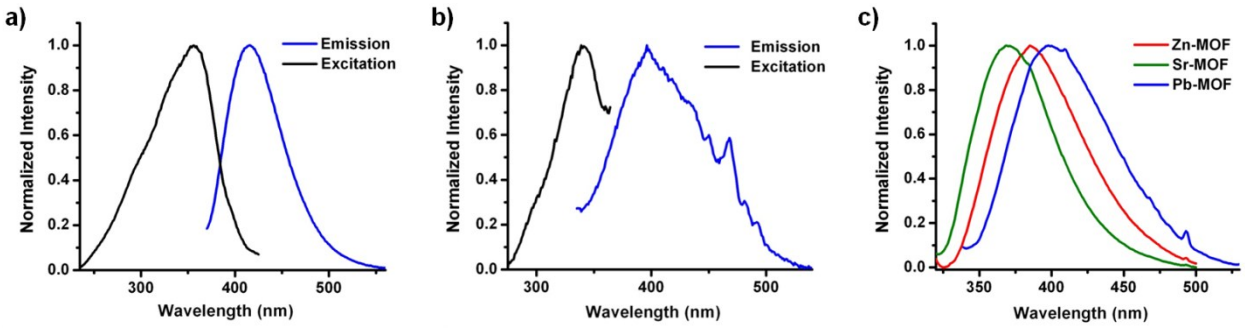

Figure S7. (a) Excitation and emission spectra of (a) the tetraacid ligand $\mathbf{H_4L}$ in the solid state and (b) the parent **Cd-MOF**. (c) Emission spectra of **Zn-MOF**, **Sr-MOF** and **Pb-MOF**, accessed by PSME of **Cd-MOF** (λ_{ex}= 300 nm.).

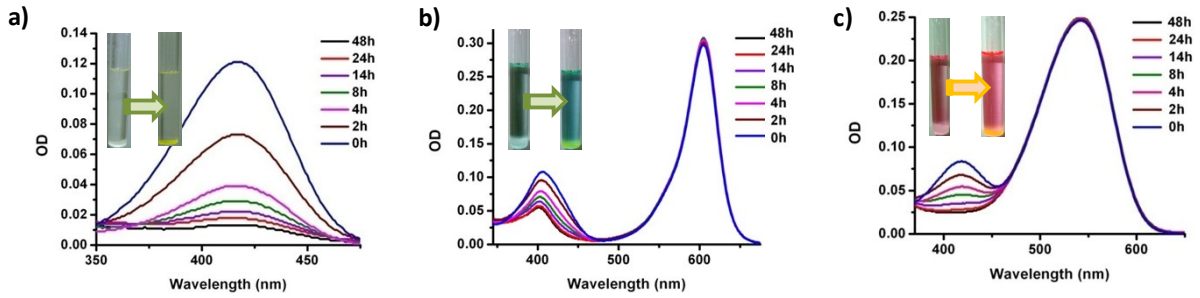

Figure S8. Adsorption (a) of the cationic dye TT in DMF with the anionic **Cd-MOF** as monitored by UV-vis spectroscopy, selective adsorption of TT by the **Cd-MOF** in the presence of negative dye XyCy (b) and neutral dye NR (c).

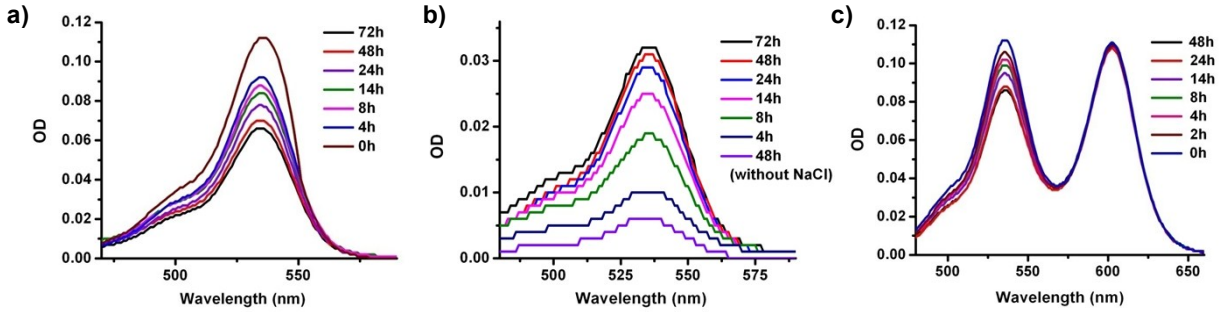

Figure S9. Adsorption (a) and subsequent release–upon treatment with saturated solution of NaCl–of the cationic dye Rhodamine-6G (Rh-6G) in DMF with the anionic **Cd-MOF** as monitored by UV-vis spectroscopy (b). (c) Competitive adsorption of Rh-6G by **Cd-MOF** in the presence of an anionic dye, namely, bromophenol blue.

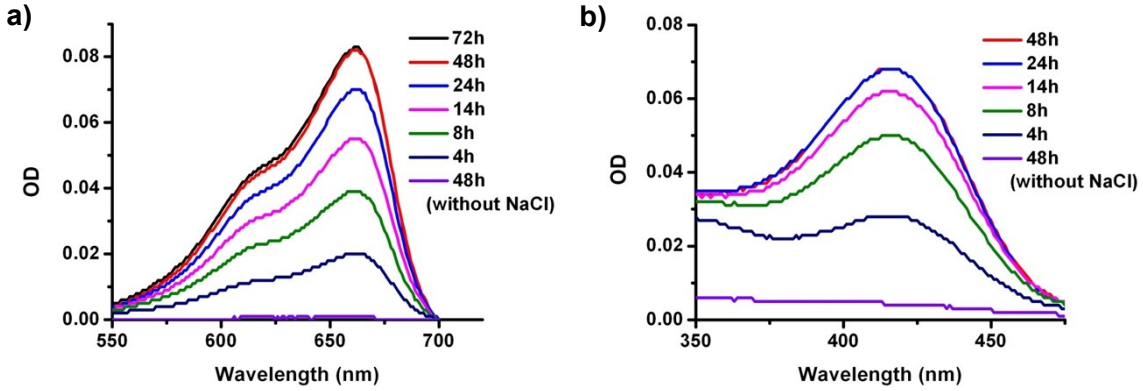

Figure S10. Reversion of dye adsorption: (a) MB and (b) TT from the **Cd-MOF** upon treatment with a saturated solution of NaCl in DMF, as monitored by UV-vis spectroscopy.

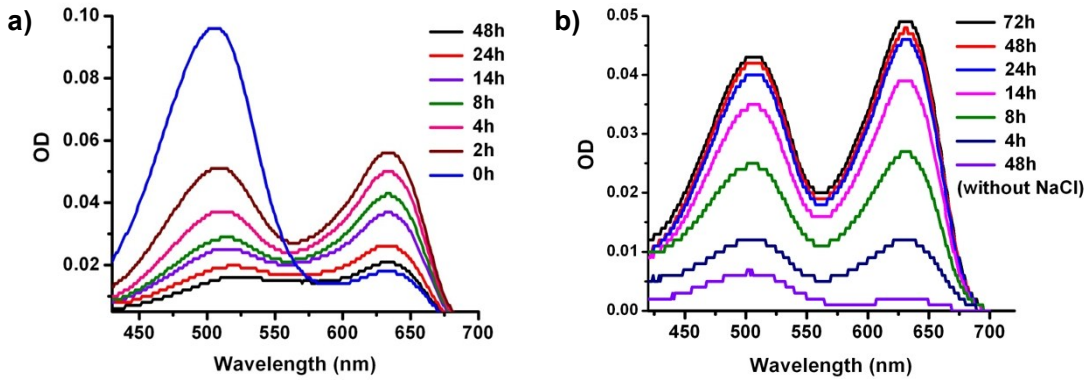

Figure S11. Adsorption of the cationic dye Nile blue by **Cd-MOF** (a), and subsequent release upon treatment with saturated solution of NaCl in DMF, as monitored by UV-vis spectroscopy (b).

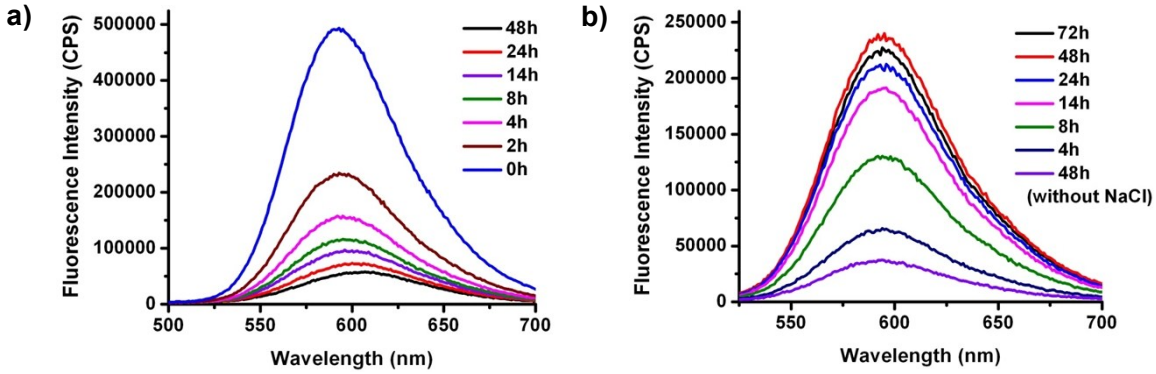

Figure S12. Adsorption of the cationic dye NB with **Cd-MOF** (a), and (b) its subsequent release upon treatment with saturated solution of NaCl in DMF, as monitored by change in the fluorescence intensity of the supernatant solution with time (b).

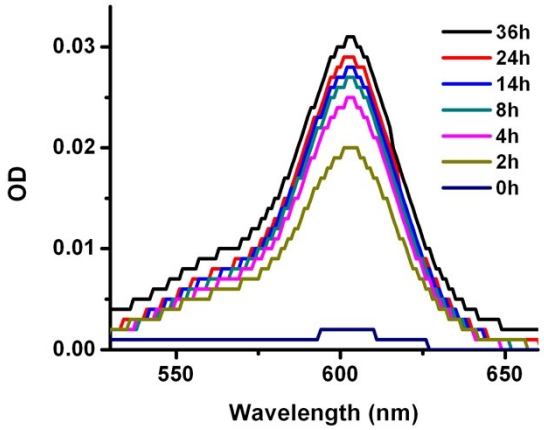

Figure S13. Release experiment of BB from the **Eu@MOF**, as monitored by UV-vis spectroscopy.

Table S3. Crystallographic parameters for **Cd-MOF1, Cd-MOF2, Cd-MOF4 and Cd-MOF8**.

MOF	**Cd-MOF1**	**Cd-MOF2**	**Cd-MOF4**	**Cd-MOF8**
Empirical formula	$C_{88}H_{60}O_{24}Cd_3$	$C_{88}H_{60}Cd_3O_{24}$	$C_{88}H_{60}O_{24}$ Cd_3	$C_{112}H_{116}N_8O_{34}$ Cd_4
Formula weight	1838.59	1838.59	1838.56	2567.72
Temperature (K)	100(2) K	100(2) K	100(2) K	100(2) K
Wavelength (Å)	0.71073 Å	0.71073 Å	0.71073 Å	0.71073 Å
Crystal system	Triclinic	Triclinic	Triclinic	Triclinic
Space group	P -1	P -1	P -1	P -1
Unit cell dimensions	a = 15.462(5) Å b = 16.063(5) Å c = 18.103(5) Å α= 107.120(5)° β= 102.556(5)° γ = 111.229(5)°	a = 15.277(2) Å b = 16.131(2) Å c = 17.297(3) Å α= 67.016(3)° β= 81.847(3)° γ = 62.703(2)°	a = 16.1904(18) Å b = 18.127(2) Å c = 27.495(3) Å α= 75.967(2)° β= 88.446(2)° γ = 72.710(2)°	a = 15.4562(18) Å b = 16.278(2) Å c = 18.346(2) Å α= 108.559(2)° β= 103.799(2)° γ = 108.453(2)°
Volume ($Å^3$)	3731	3483.6(9)	7466.0(14)	3844.0(8)
Z, Calculated density(g/cm^3)	1, 0.865	1, 0.876	2, 0.818	1, 1.109
Absorption coefficient(mm^{-1})	0.604	0.499	0.465	0.607
F(000)	964	924	1848	1308
θ range for data collection (°)	2.291 to 28.399°	1.280 to 28.387°	0.764 to 28.348°	1.264 to 28.306°
Limiting indices	-20<=h<=20 -21<=k<=15 -23<=l<=24	-20<=h<=13 -21<=k<=16 -22<=l<=14	-21<=h<=21 -23<=k<=23 -19<=l<=35	-9<=h<=19 -20<=k<=19 -24<=l<=24
Reflections collected	28367	21432	47079	23842
Independent reflections	17923 [R(int) = 0.0672]	15202 [R(int) = 0.0368]	32975 [R(int) = 0.0628]	16857 [R(int) = 0.0338]
Completeness to *θ*	97.2 %	97.8 %	98.3 %	98.1 %
Refinement method	Full-matrix least-squares on F^2	Full-matrix least-squares on F^2	Full-matrix least-squares on F^2	Full-matrix least-squares on F^2
Data / restraints / parameters	17923 / 0 / 366	15202 / 0 / 470	32975 / 0 / 976	16857 / 9 / 572
Goodness-of-fit on F^2	0.912	0.934	1.046	1.134
Final *R* indices [$I > 2\sigma(I)$]	R1 = 0.1328 wR2 = 0.3375	R1 = 0.0724 wR2 = 0.1936	R1 = 0.1024 wR2 = 0.2452	R1 = 0.1026 wR2 = 0.2769
R indices (all data)	R1 = 0.1328 wR2 = 0.3375	R1 = 0.1198 wR2 = 0.2286	R1 = 0.1690 wR2 = 0.2718	R1 = 0.1407 wR2 = 0.3398
Largest diff. peak and hole ($e.Å^{-3}$)	2.421 and -2.549	1.155 and -2.372	5.400 and -1.638	3.684 and -3.796

Table S4. Crystallographic parameters for **Cd-MOF12**, **Ca@MOF**, **La@MOF** and **Pr@MOF.**

MOF	**Cd-MOF12**	**Ca@MOF**	**La@MOF**	**Pr@MOF**
Empirical formula	$C_{97}H_{82}N_3O_{30}Cd_4$	$C_{88}H_{60}O_{29}Ca_{1.75}Cd_{2.25}$	$C_{91}H_{67}NO_{26}Cd_{1.46}La_{1.54}$	$C_{97}H_{81}N_3O_{27}Cd_{1.43}Pr_{1.57}$
Formula weight	2219.3	1904.32	1968.53	2102.71
Temperature (K)	100(2) K	100(2) K	100(2) K	100(2) K
Wavelength (Å)	0.71073 Å	0.71073 Å	0.71073 Å	0.71073 Å
Crystal system	Triclinic	Triclinic	Triclinic	Triclinic
Space group	P -1	P -1	P -1	P -1
Unit cell dimensions	a = 15.6469(17) Å b = 18.471(2) Å c = 27.450(3) Å α= 99.525(2)° β= 90.063(2)° γ = 103.876(2)°	a = 15.631(5) Å b = 18.456(6) Å c = 27.517(10) Å α= 80.164(7)° β= 89.994(7)° γ = 76.264(6)°	a = 15.744(3) Å b = 18.343(3) Å c = 28.121(5) Å α= 104.422(3)° β= 92.252(3)° γ = 108.122(3)°	a = 15.890(5) Å b = 18.596(6) Å c = 28.500(10) Å α= 101.979(6)° β= 94.414(6)° γ = 108.931(5)°
Volume ($Å^3$)	7588.8(14)	7591(4)	7415(2)	7697(4)
Z, Calculated density(g/cm^3)	2, 0.966	2, 0.907	2, 0.899	8, 0.925
Absorption coefficient(mm^{-1})	0.604	0.499	0.894	0.982
F(000)	2222	2096	1996	2154
θ range for data collection (°)	0.753 to 28.367°	1.154 to 28.401°	0.754 to 28.325°	1.194 to 28.297°
Limiting indices	-20<=h<=20 -24<=k<=12 -33<=l<=35	-20<=h<=19 -23<=k<=24 -35<=l<=30	-19<=h<=20 -22<=k<=23 -25<=l<=37	-20<=h<=13 -24<=k<=23 -33<=l<=37
Reflections collected	47106	46096	44502	42687
Independent reflections	33384 [R(int) = 0.0582]	33043 [R(int) = 0.0917]	31902 [R(int) = 0.0427]	32008 [R(int) = 0.0577]
Completeness to *θ*	97.9 %	97.7 %	97.6 %	95.8 %
Refinement method	Full-matrix least-squares on F^2	Full-matrix least-squares on F^2	Full-matrix least-squares on F^2	Full-matrix least-squares on F^2
Data / restraints / parameters	33384 / 0 / 1105	33043 / 0 / 1077	31902 / 0 / 1016	32008 / 0 / 835
Goodness-of-fit on F^2	0.949	0.803	0.981	0.932
Final *R* indices [$I > 2\sigma(I)$]	R1 = 0.0903 wR2 = 0.2242	R1 = 0.1094 wR2 = 0.2623	R1 = 0.0823 wR2 = 0.2128	R1 = 0.1115 wR2 = 0.2906
R indices (all data)	R1 = 0.1528 wR2 = 0.2730	R1 = 0.2188 wR2 = 0.2992	R1 = 0.1254 wR2 = 0.2548	R1 = 0.1687 wR2 = 0.3365
Largest diff. peak and hole ($e.Å^{-3}$)	3.268 and -2.815	2.147 and -1.638	1.749 and -2.213	3.419 and -3.001

Table S5. Crystallographic parameters for **Nd@MOF**, **Sm@MOF**, **Eu@MOF** and **Tb@MOF.**

MOF	**Nd@MOF**	**Sm@MOF**	**Eu@MOF**	**Tb@MOF**
Empirical formula	$C_{97}H_{81}N_3O_{28}Cd_{1.33}Nd_{1.67}$	$C_{104}H_{104}N_6O_{29}Cd_{1.72}Sm_{1.28}$	$C_{97}H_{81}N_3O_{27}Cd_{1.68}Eu_{1.32}$	$C_{88}H_{60}O_{26}Tb_3$
Formula weight	2127.13	2287.86	2110.18	2010.15
Temperature (K)	100(2) K	100(2) K	100(2) K	100(2) K
Wavelength (Å)	0.71073 Å	0.71073 Å	0.71073 Å	0.71073 Å
Crystal system	Triclinic	Triclinic	Triclinic	Triclinic
Space group	P -1	P -1	P -1	P -1
Unit cell dimensions	a = 15.785(2) Å b = 18.275(3) Å c = 28.066(4) Å α= 104.478(3)° β= 92.048(3)° γ = 107.860(3)°	a = 15.813(4) Å b = 18.213(4) Å c = 27.961(6) Å α= 104.736(4)° β= 91.538(4)° γ = 107.955(4)°	a = 15.970(2) Å b = 18.597(3) Å c = 28.434(4) Å α= 100.536(2)° β= 95.130(2)° γ = 109.615(2)°	a = 15.779(8) Å b = 18.369(9) Å c = 28.064(14) Å α= 103.419(9)° β= 91.978(7)° γ = 108.705(8)°.
Volume (Å^3)	7405.6(19)	7360(3)	7716.2(19)	7442(6)
Z, Calculated density(g/cm^3)	2, 0.969	2, 1.061	2, 0.936	2, 0.906
Absorption coefficient(mm^{-1})	1.086	1.237	1.252	1.454
F(000)	2158	2374	2174	2006
θ range for data collection (°)	0.755 to 28.331°	0.758 to 28.373°	2.04 to 21.20°	1.211 to 28.296°
Limiting indices	-18<=h<=20 -23<=k<=2 -36<=l<=26	-21<=h<=9 -21<=k<=23 -37<=l<=35	-16<=h<=16 -16<=k<=18 -28<=l<=28	-19<=h<=20 -24<=k<=24 -20<=l<=37
Reflections collected	46281	44824	28723	43102
Independent reflections	32513 [R(int) = 0.0339]	32018 [R(int) = 0.0462]	16735 [R(int) = 0.0385]	31641 [R(int) = 0.1972]
Completeness to *θ*	98.0 %	97.8 %	98.2 %	
Refinement method	Full-matrix least-squares on F^2	Full-matrix least-squares on F^2	Full-matrix least-squares on F^2	Full-matrix least-squares on F^2
Data / restraints / parameters	32513 / 0 / 977	32018 / 0 / 1175	16735 / 0 / 1041	31641 / 0 / 410
Goodness-of-fit on F^2	1.168	1.025	1.091	1.014
Final *R* indices [$I > 2\sigma(I)$]	R1 = 0.1061 wR2 = 0.2928	R1 = 0.1014 wR2 = 0.2695	R1 = 0.0972 wR2 = 0.2590	R1 = 0.2057 wR2 = 0.4474
R indices (all data)	R1 = 0.1427 wR2 = 0.3546	R1 = 0.1648 wR2 = 0.3159	R1 = 0.1123 wR2 = 0.2695	R1 = 0.4734 wR2 = 0.5884
Largest diff. peak and hole (e.Å^{-3})	4.580 and -2.909	2.313 and -2.489	3.113 and -3.224	2.663 and -0.936

Table S6. Crystallographic parameters for **Mn@MOF**, **Co@MOF**, **Cu@MOF** and **Zn@MOF.**

MOF	**Mn@MOF**	**Co@MOF**	**Cu@MOF**	**Zn@MOF**
Empirical formula	$C_{44}H_{30}O_{12}Mn_{0.63}Cd_{0.87}$	$C_{44}H_{30}O_{12}Co_{1.21}Cd_{0.29}$	$C_{94}H_{74}N_2O_{30}Cu_{3.3}Cd_{0.69}$	$C_{44}H_{30}O_{12}Zn_{1.46}Cd_{0.04}$
Formula weight	833.15	3749(2)	1999.37	850.74
Temperature (K)	100(2) K	100(2) K	100(2) K	100(2) K
Wavelength (Å)	0.71073 Å	0.71073 Å	0.71073 Å	0.71073 Å
Crystal system	Triclinic	Triclinic	Triclinic	Triclinic
Space group	P -1	P -1	P -1	P -1
Unit cell dimensions	a = 15.957(4) Å b = 16.460(4) Å c = 17.300(5) Å α= 106.070(6)° β= 100.850 (5)° γ = 113.408(5)°	a = 15.468(5) b = 15.785(5) c = 18.038(6) α= 107.270(6)° β= 103.949(6)° γ = 107.163(5)°	a = 15.508(3) Å b = 16.241(3) Å c = 18.383(4) Å α= 108.709(4)° β= 104.279(4)° γ = 107.160(4)°	a = 15.116(5) Å b = 15.393(5) Å c = 18.225(6) Å α= 105.732(6)° β= 106.553(6)° γ = 104.405(7)°
Volume ($Å^3$)	3770.9(17)	3749(2)	3880.8(13)	3660(2)
Z, Calculated density(g/cm^3)	2, 0.734	2, 0.743	1, 0.842	2, 0.770
Absorption coefficient(mm^{-1})	0.289	0.370	0.589	0.530
F(000)	855	861	1010	870
θ range for data collection (°)	1.464 to 28.249°.	1.471 to 28.159°	1.450 to 28.240°	1.254 to 28.371°.
Limiting indices	-18<=h<=20 -21<=k<=21 -22<=l<=15	-14<=h<=20 -19<=k<=19 -23<=l<=14	-11<=h<=20 -21<=k<=20 -23<=l<=18	-20<=h<=19 -8<=k<=20 -24<=l<=24
Reflections collected	19658	19883	23659	22314
Independent reflections	14714 [R(int) = 0.1442]	15439 [R(int) = 0.0577]	16824 [R(int) = 0.0397]	16003 [R(int) = 0.0768]
Completeness to θ	91.4 %	95.8 %	97.6 %	
Refinement method	Full-matrix least-squares on F^2	Full-matrix least-squares on F^2	Full-matrix least-squares on F^2	Full-matrix least-squares on F^2
Data / restraints / parameters	14714 / 0 / 231	15439 / 0 / 501	16824 / 0 / 513	16003 / 0 / 513
Goodness-of-fit on F^2	1.917	0.734	1.300	0.836
Final *R* indices [$I > 2\sigma(I)$]	R1 = 0.4089 wR2 = 0.6100	R1 = 0.0933 wR2 = 0.2232	R1 = 0.1456 wR2 = 0.3555	R1 = 0.1016 wR2 = 0.2376
R indices (all data)	R1 = 0.4768 wR2 = 0.6778	R1 = 0.1840 wR2 = 0.2603	R1 = 0.1791 wR2 = 0.4066	R1 = 0.2061 wR2 = 0.2719
Largest diff. peak and hole ($e.Å^{-3}$)	5.440 and -1.294	0.682 and -0.941	4.434 and -2.691	0.727 and -1.297

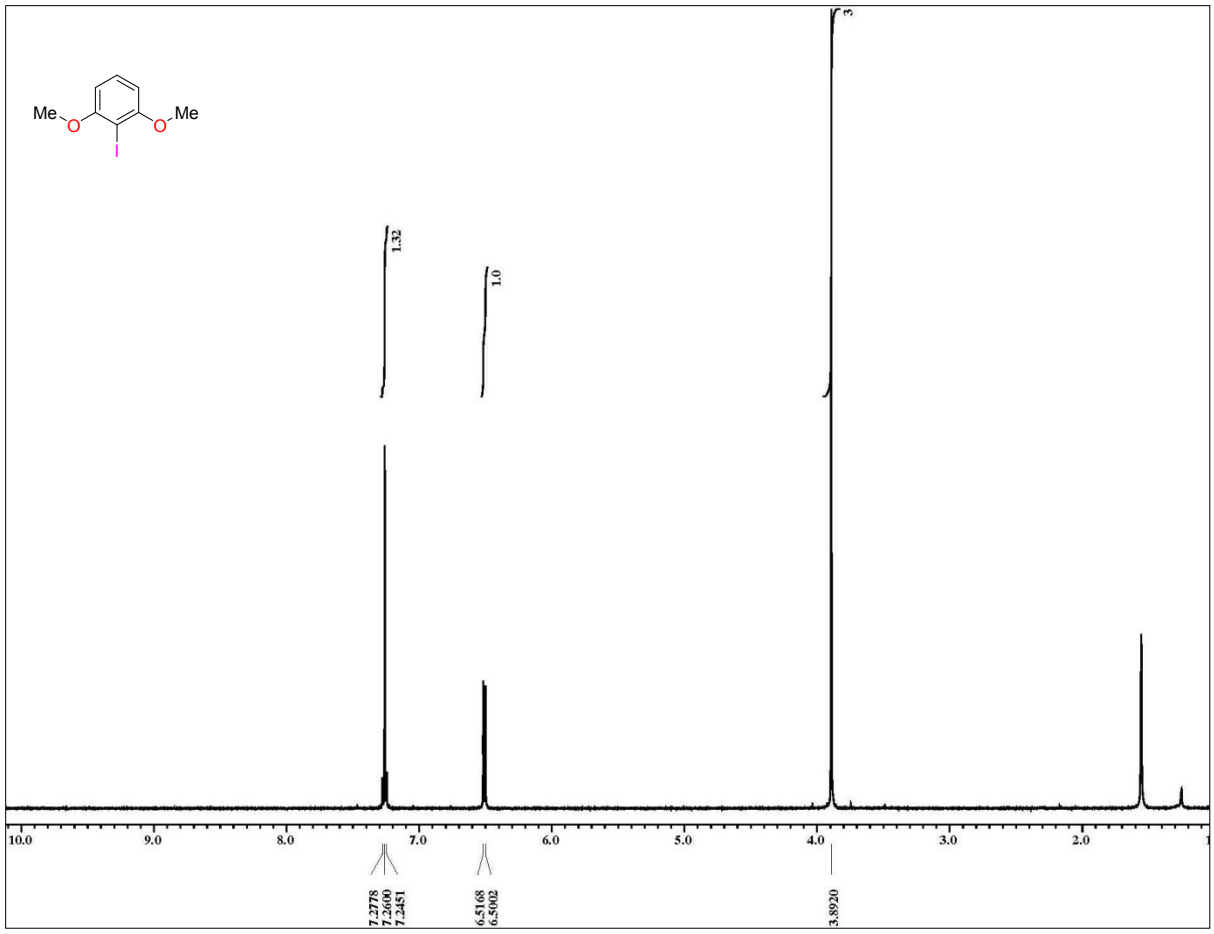

Figure S14. ^{1}H NMR spectrum (500 MHz) of 2-iodo-1,3-dimethoxybenzene in $CDCl_3$.

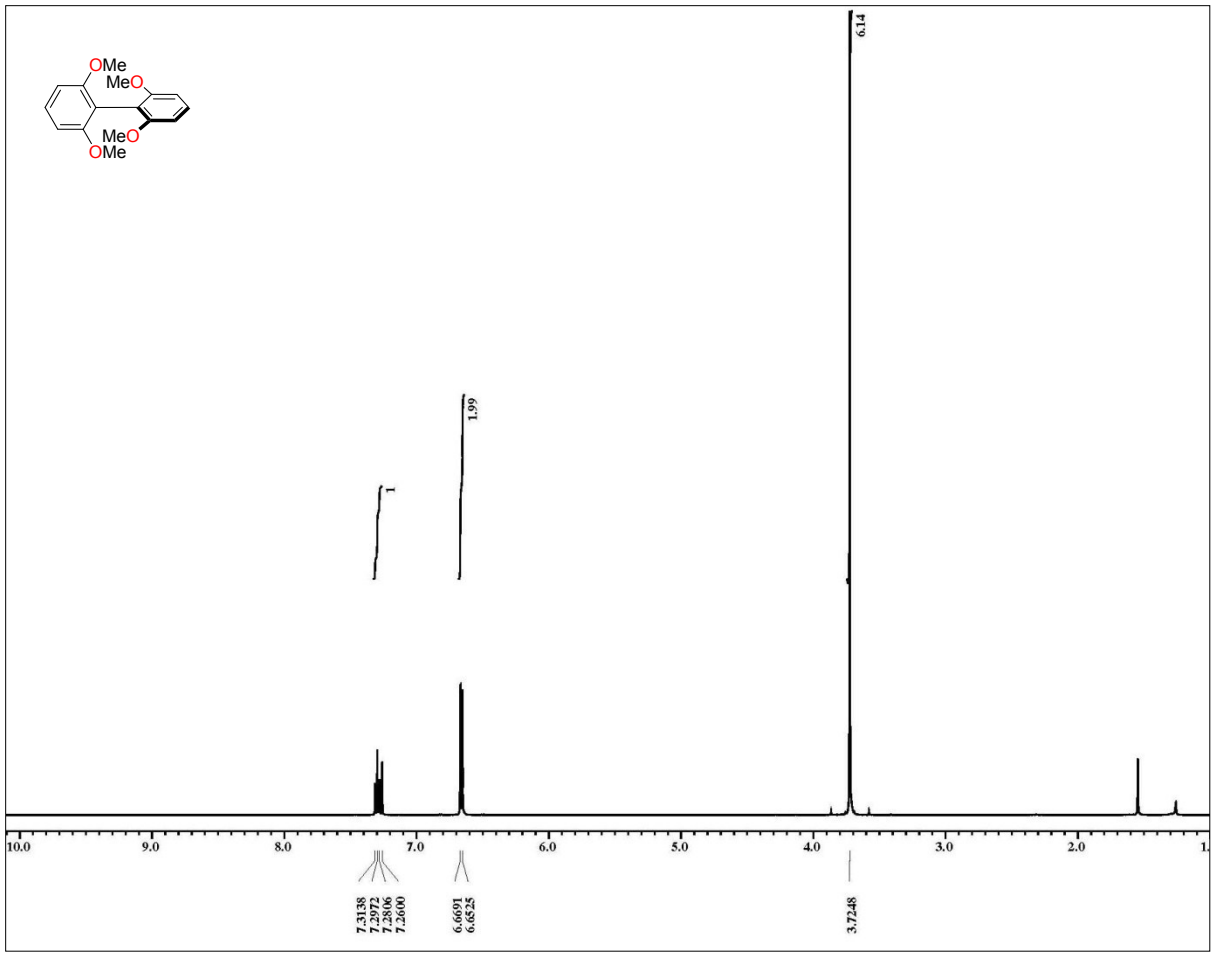

Figure S15. ^{1}H NMR spectrum (500 MHz) of 2,2',6,6'-tetramethoxy-1,1'-biphenyl in $CDCl_3$.

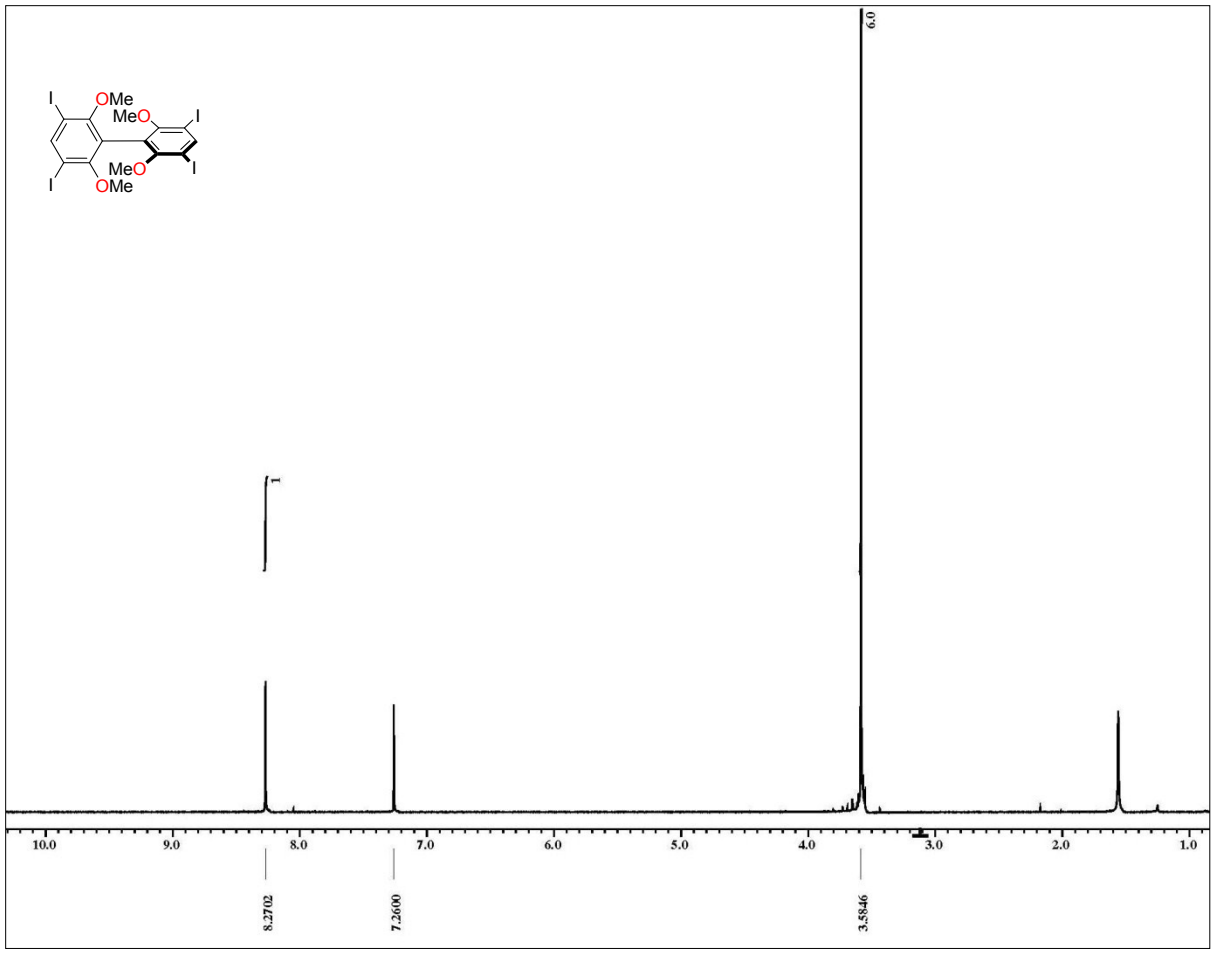

Figure S16. ^{1}H NMR spectrum (500 MHz) of 3,3',5,5'-tetraiodo-2,2',6,6'-tetramethoxy-1,1'-biphenyl in $CDCl_3$.

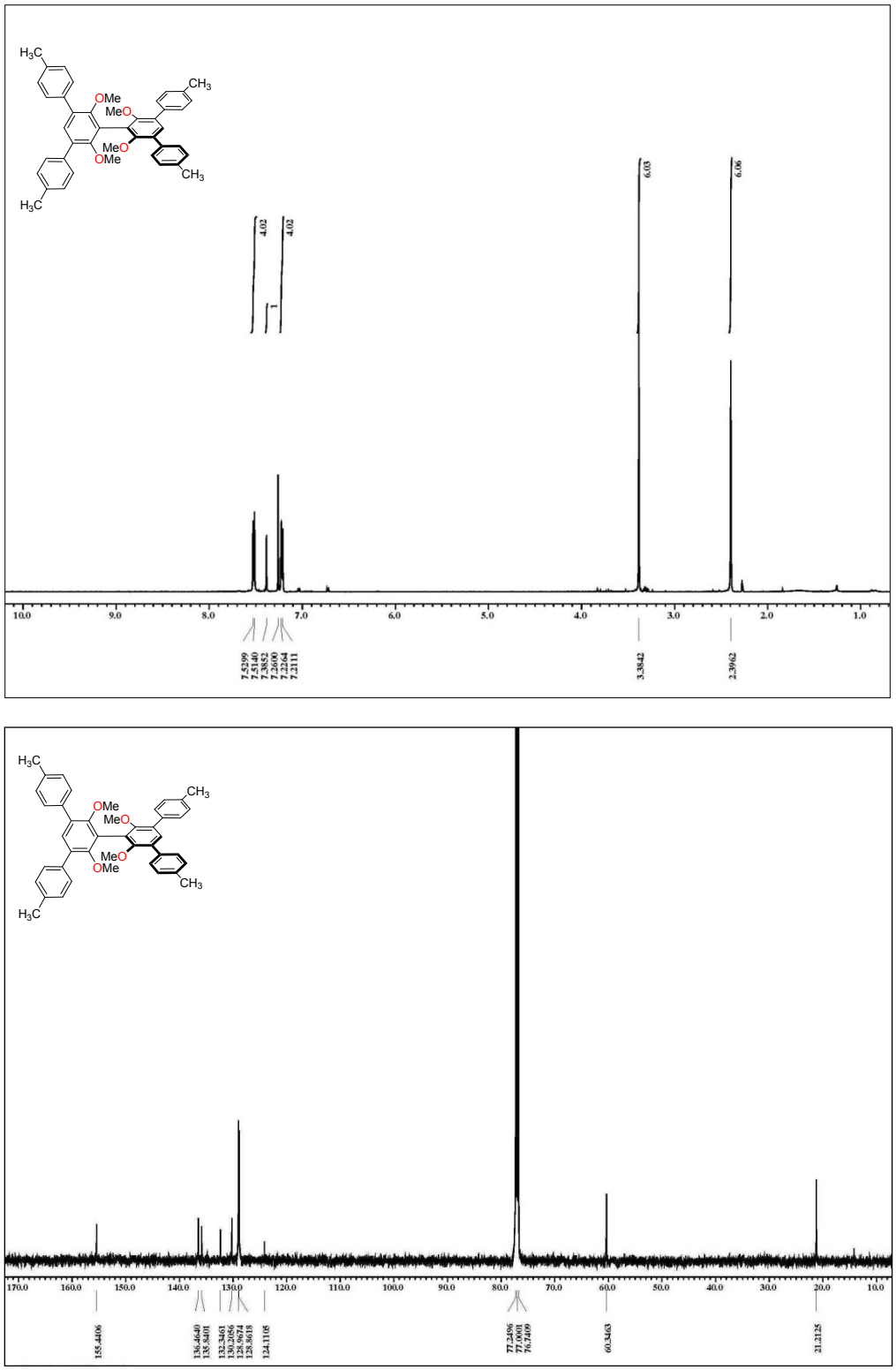

Figure 17. ^{1}H (500 MHz) and ^{13}C NMR (125 MHz) spectra of 3,3',5,5'-tetrakis(*p*-methylphenyl)-2,2',6,6'-tetramethoxy-1,1'-biphenyl in $CDCl_3$.

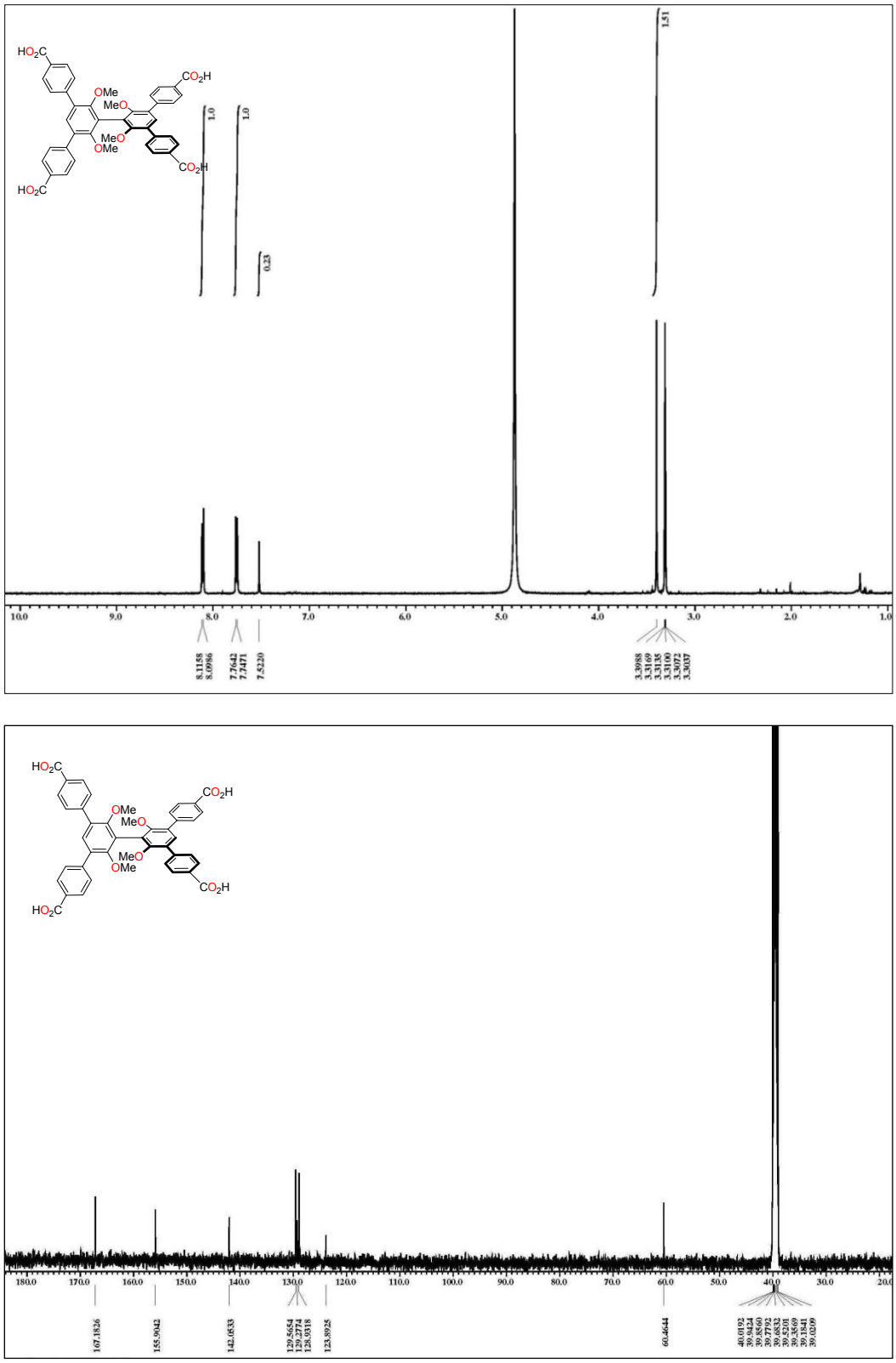

Figure 18. ^{1}H (500 MHz) and ^{13}C (125 MHz) NMR spectra of 3.3',5,5'-tetrakis(*p*-carboxyphenyl)-2,2',6,6'-tetramethoxy-1,1'-biphenyl in CD_3OD and DMSO-d_6, respectively.